Canadian Mineralogist
Vol. 14, pp. 322-333 (1976)

PEKOITE, $CuPbBi_{11}S_{18}$, A NEW MEMBER OF THE BISMUTHINITE-AIKINITE MINERAL SERIES: ITS CRYSTAL STRUCTURE AND RELATIONSHIP WITH NATURALLY- AND SYNTHETICALLY-FORMED MEMBERS

W. G. MUMME AND J. A. WATTS
CSIRO Division of Mineral Chemistry, P.O. Box 124, Port Melbourne, Victoria 3207, Australia

ABSTRACT

The crystal structure of pekoite, ideally $CuPbBi_{11}(S,Se)_{18}$, a new mineral from the Juno mine at Tennant Creek, N.T., Australia, has been determined from a three-dimensional X-ray analysis and refined to give an *R*-value of 0.12. Pekoite has the space group $P2_1am$, with a 11.472, b 3×11.248, c 4.016Å for the composition $Cu_{.65}Pb_{.78}Bi_{11.5}S_{14.93}Se_{3.07}$. The structure is a three-fold superstructure based on bismuthinite and is made up of two slabs of bismuthinite (Bi_4S_6) ribbons and one slab of krupkaite ($CuPbBi_3S_6$) ribbons alternating along the *b*-axis. The classification of the ordered mineral phases which form along the Bi_2S_3-$CuPbBiS_3$ composition line is discussed, together with a study of the crystal structure of members of the series synthetically prepared at 450-500°C. The results of single-crystal analysis of the synthetic compounds confirm that, in contrast to the ordered natural members, complete solid solution does occur between Bi_2S_3 and $CuPbBiS_3$, with copper and lead atoms progressively filling the sites which they fully occupy in the end-member aikinite.

SOMMAIRE

La structure cristalline du pékoite, un nouveau minéral $CuPbBi_{11}(S,Se)_{18}$, provenant de la mine Juno de Tennant Creek, N.T., Australie, a été déterminée par une analyse tridimensionnelle par diffraction des rayons-X et affinée afin d'obtenir un indice *R* de 0.12. Sa maille élémentaire est $P2_1am$, dont a 11.472, b 3×11.248, c 4.016Å et de composition $Cu_{.65}Pb_{.78}Bi_{11.5}S_{14.93}Se_{3.07}$. Sa structure est en fait une superstructure de l'ordre de 3, composée principalement de bismuthinite: deux plaques de bismuthinite (Bi_4S_6) et une plaque de krupkaite ($CuPbSi_3S_6$) alternent le long de l'axe-*b*. On discute de la classification des phases minérales ordonnées qui se trouvent dans le système Bi_2S_3-$CuPbBiS_3$, et d'une étude de la structure cristalline des membres de la série préparés par synthèse à 450-500°C. Les résultats de l'analyse de cristaux uniques des composés synthétiques confirment qu'il y a effectivement une solution solide complète entre Bi_2S_3 et $CuPbBiS_3$, contrairement à ce que l'on trouve pour les exemples naturels ordonnés. Les atomes de cuivre et de plomb remplissent progressivement les sites et les occupent complètement dans le pôle extrême, l'aikinite.

(Traduit par le journal)

INTRODUCTION

Recent developments in the study of the minerals in the system bismuthinite-aikinite are found in Mumme *et al.* (1976) and Harris & Chen (1976). The history leading up to these studies is that Moore's (1967) classification based on Welin's (1966) studies was questioned by Zak *et al.* (1975) and Synecek & Hybler (1975) after these workers discovered a new intermediate member krupkaite, $CuPbBi_3S_6$, and found that its crystal structure failed to conform with Moore's Z^* classification. Synecek & Hybler (1975) proposed a new nomenclature which, however, had the deficiency that their classification symbol, Z_x, could be common to several intermediate members. Also, their classification incorrectly predicted the space group of Welin's "new" member $Cu_3Pb_3Bi_7S_{15}$ to be *Pbnm*, not $Pb2_1m$ as was already known.

Independently of Zak *et al.*, the failure of Moore's classification was also recognized by Mumme *et al.* (1976) through the results of separate concurrent studies of the structures of krupkaite (Mumme 1975), and another previously unrecorded member of the series, pekoite, now presented in this paper. Both of these minerals were discovered in the Juno mine at Tennant Creek, Australia (Large & Mumme 1975).

Mumme *et al.* proposed that the classification of the minerals should rest on the establishment of distinct names for the ordered mineral species. As part of this proposed nomenclature, which has since been approved by the IMA, Welin's $Cu_3Pb_3Bi_7S_{15}$ phase came to be called lindstromite,* and the individual members known as bismuthinite derivatives.

Most recently, Harris & Chen (1976) independently studied the six phases classified by Mumme *et al.* and showed that all except lindstromite possess considerable solid-solution ranges. This type of behavior for pekoite is also exemplified in the results described in this present paper.

*Proposed by Professor B. J. Wuensch.

The crystal structure of pekoite was recognized to be extremely important to an understanding of the relationships among the members of this mineral series, and is reported here in detail. The present investigation has also been extended to a study of possible superstructure formation in synthetic members of the series prepared by solid-state reactions.

The Crystal Structure of Pekoite

Experimental

Members of the bismuthinite-aikinite series are common in the No. 1 and No. 2 orebodies at the Juno mine, Tennant Creek (Large 1974). Most of the members studied contain oriented blebs which resemble exsolution textures (Fig. 1), and may be straight or cymoidal. Microprobe analyses (Large & Mumme 1975) which suggested that the blebs are members of the bismuthinite-aikinite series with a higher lead and copper content than the host grains are plotted in Figure 2. The Pb content of the blebs was about 14%, which corresponded well with the mineral gladite, $CuPbBi_5S_9$. The analyses for the host material (Table 2) although rather more scattered, corresponded to the composition $CuPbBi_{11}S_{18}$ with a lead content of about 6%.

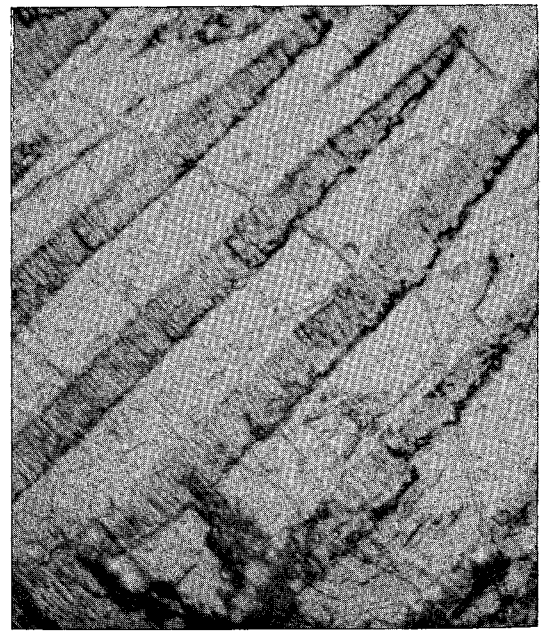

FIG. 1. Exsolution textures developed in members of the bismuthinite-aikinite series from the Juno mine. Host=pekoite; intergrown phase=gladite. Etched with HBr for 60 sec. The field is 50 μm wide.

X-ray Weissenberg photographs of small aligned fragments of material showing the exsolution textures gave results similar to those shown in Figure 3. Reflections on the Weissenberg films gradually split into two with increasing values of h only. Two lattices aligned in a parallel fashion are present, and the fragments investigated thus consist of two submicroscopically intergrown minerals as already sug-

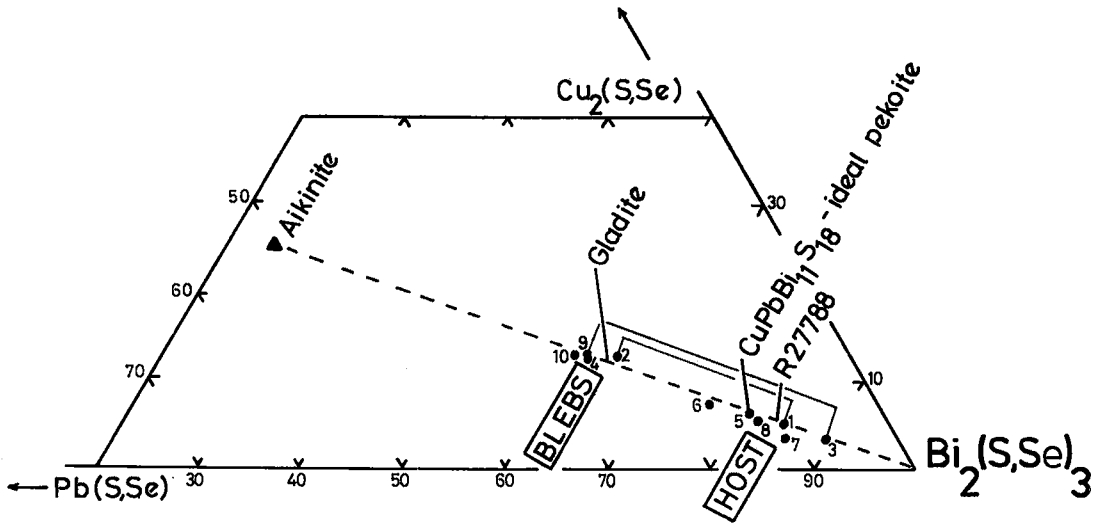

FIG. 2. Microprobe analyses of the intergrowth phases pekoite and gladite (from Large & Mumme 1975) together with that of the pekoite specimen (R27788) studied in this paper. Compositions are plotted in the $Bi_2(S,Se)_3$, Pb(S,Se), $Cu_2(S,Se)$ system. Exsolution pairs are joined by lines.

TABLE 1. CRYSTALLOGRAPHIC DATA FOR PEKOITE, $CuPbBi_{11}(S,Se)_{18}$

Mineral	Composition	Lattice constants (Å)			Space group	Reference
Pekoite	$CuPbBi_{11}S_{14}Se_4$	b=3x11.248(2)	a=11.472(2)	c=4.016(1)	$P2_1am$	This study
Pekoite	$CuPbBi_{11}S_{18}$	b=3x11.168(2)	a=11.322(2)	c=3.987(1)	$P2_1am$	This study
Gladite	$CuPbBi_5S_9$	b=3x11.177(2)	a=11.486(2)	c=4.003	$Pnma$	Kohatsu & Wuensch (1973)
		b=3x11.182(2)	a=11.498(2)	c=4.001	$Pnma$	This study

gested by the microprobe results. Furthermore, the Weissenberg results show that the blebs and host may have parallel orientation. The two minerals are orthorhombic, with identical values of b and c, but differ slightly in a (setting $b>a>c$). The refined unit-cell parameters derived from the Guinier powder data (calibrated with KCl, a_o = 6.2929Å) are given in Table 1. Superlattice reflections present on the Weissenberg films show that both of the minerals are superstructures based upon bismuthinite, with one lattice constant equal to three times that of the corresponding translation in bismuthinite. The blebs have lattice parameters nearly identical with those of gladite, whereas the host mineral has subcell dimensions substantially larger than that of bismuthinite and a composition close to $CuPbBi_{11}S_{18}$, this mineral now being known as pekoite. This name, for which IMA approval was granted in July, 1975, is after the Peko mine, one of the first in the Tennant Creek gold field.

TABLE 2. MICROPROBE ANALYSIS OF PEKOITE IN SPECIMEN R27788

	wt. %	Molecular Proportions Based on 18(S+Se)	
Bi	73.6	Bi	11.50
Pb	5.1	Pb	0.78
Cu	1.3	Cu	0.65
S	14.3	S + Se	18.
Se	7.4		
Total	101.7		

Jeol JXA-SOA microprobe, 25KV. Standards used: galena, claustha-lite, Bi and Cu metals. The correction program, MAGIC IV, was developed by J.W. Colby of Bell Telephone Inc., Allantown, Pennsylvania.

The crystal structure of gladite had been reported by Kohatsu & Wuensch (1973), but the pekoite intimately intergrown with it represented a previously unrecognized new member of the Bi_2S_3-$CuPbBiS_3$ series. It was initially thought that the study of its crystal structure would have to be attempted using X-ray data collected from a fragment of this material which exhibited exsolution lamellae, in a somewhat similar fashion to that used in Synecek & Hybler's (1974) studies of krupkaite and gladite. However, other specimens from Tennant Creek (R27798 and R27788)* were found to contain this new member with selenium contents up to 7% (Table 2). Crystals of pekoite from R27788

*Numbering refers to specimens presently held at Mineral Chemistry, CSIRO.

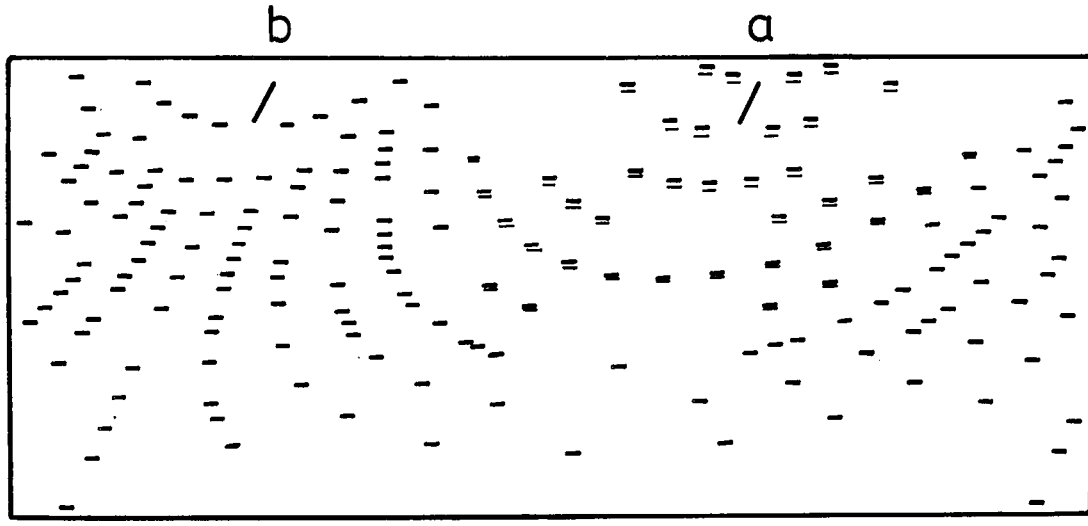

FIG. 3. Tracing of Weissenberg diagram — zero level, Cu$K\alpha$-radiation. Upper lines are pekoite α_1-reflections, lower lines are gladite α_1-reflections. The reflections separate with increasing value of h. No α_2-reflections are plotted.

gave X-ray data which showed them to be single-phase, and confirmed the three-fold cell relationship with respect to bismuthinite. The space group of pekoite was not *Pnma* (that of gladite) but $P2_1am$, that is, the same space group as krupkaite and lindstromite. The other space-group alternatives, *Pma*2 and *Pmam*, may be discounted on the basis of the substructure-superstructure relationships for similar reasons as those already described in the accounts of the crystal structure of krupkaite (Zak *et al.* 1975; Mumme 1975).

X-ray data for the levels $l = 0, 1, 2$ were collected by the multiple-film technique from a crystal of pekoite measuring .06×.06×.25 mm. The integrated equi-inclination method was used with Cu$K\alpha$ radiation. Intensities were measured visually against a standard scale. Of the 425 reflections recorded, 51 were superlattice reflections.

Solution and refinement of the structure

As the X-ray data showed a strong subcell relationship with bismuthinite, the original atomic positions used for pekoite (in each of the three subcells) were taken as those of bismuthinite, transposed by $\frac{1}{4}b$, as required for the space group $P2_1am$. The three-dimensional data were then refined using a local version of ORFLS (Busing *et al.* 1962). Previous experience in refinement of krupkaite (Mumme 1975), aikinite, and gladite (Kohatsu & Wuensch 1971, 1973) indicated that the Pb site in the structure would be characterized by a significant displacement of the location of the Pb atom relative to that of the corresponding Bi atom in the bismuthinite structure. However, the superstructure intensities were very weak, and the attempted refinement with the substructure reflections included in the data set resulted in these intense reflections dominating the parameter shifts and the atoms refined to the bismuthinite positions. At this stage, therefore, calculations were commenced to determine which of the ordered models for pekoite permitted by the subcell-superstructure relationship gave the best agreement for the superstructure reflections. Using the 51 superstructure reflections it was demonstrated that for these models the best structure factor agreement ($R=0.25$) occurred when copper occupied the site in the structure shown in Figure 4, with the adjacent lead site displaced by 0.5Å from its equivalent bismuthinite position. This, basically, is the method of key shifts which has been described by Ito (1973). The R-values obtained from similar calculations for all the other possible models varied from .36 to .52.

The final R-value for all subcell and supercell reflections was 12.1%, after absorption corrections were made for a cylindrical specimen of $\mu R=1320$. The weighting scheme used was that of Cruickshank *et al.* (1961). Final atomic parameters and bond lengths are given in Tables 3 and 4. The structure factor table has been deposited with the National Science Library, Ottawa.

Description and discussion of the structure of pekoite

The proposed ideal structure of pekoite, $CuPbBi_{11}(S,Se)_{18}$ is shown in Figure 4. As distinct from krupkaite, which is composed entirely of slabs of krupkaite-like ribbons, and gladite, which contains two krupkaite slabs and one bismuthinite slab alternating, the structure

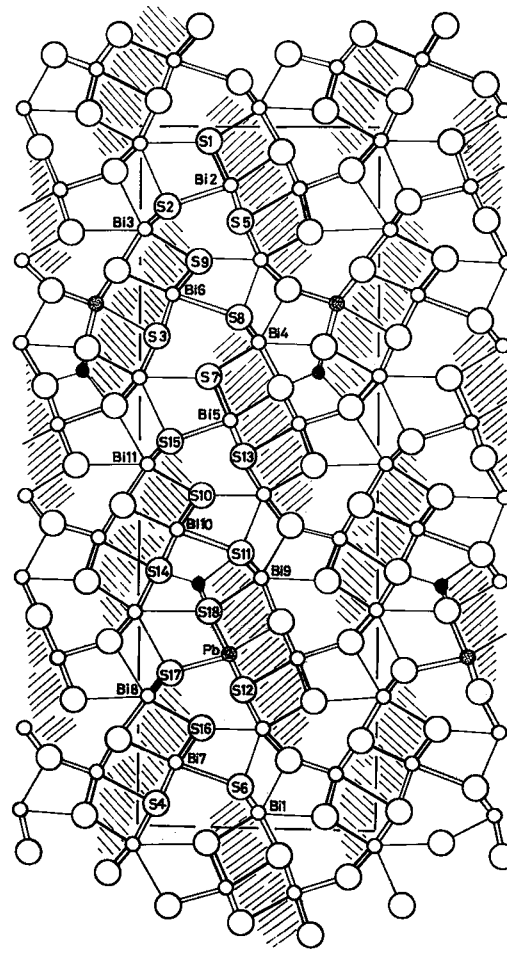

FIG. 4. Crystal structure of ideal pekoite, $CuPbBi_{11}S_{18}$ projected onto (001). The shaded portions correspond to the stibnite quadruple chain.

of pekoite has two bismuthinite slabs and one krupkaite slab alternating.

The structural relationships, and crystal chemistry of the intermediate bismuthinite derivatives, have now been discussed by Mumme *et al.* (1976) and Harris & Chen (1976), and there is no new information known to the present authors which can be added here. However, for the sake of completeness, Figure 5 summarizes, in the notation of Omassa & Nowacki (1970), the structures of the four bismuthinite derivatives studied to the present. All are composed of various combinations of bismuthinite, krupkaite and aikinite-like ribbons. Those members of the series between bismuthinite and krupkaite are composed entirely of bismuthinite and krupkaite-like ribbons. Hammarite, $Cu_2Pb_2Bi_4S_9$, and lindstromite, $Cu_3Pb_3Bi_7S_{15}$, the two other known members of the series which occur between krupkaite and aikinite, are yet to be studied, but it may be predicted that they will incorporate both the aikinite-ribbon and the krupkaite-ribbon into their structures.

TABLE 3. ATOMIC COORDINATES IN PEKOITE

Site	Occupancy	x	y	z	$B(Å)^2$
M1	Bi	.4685(4)	.9752(6)	1/2	.81(5)
M2	Bi	.3368(7)	.0710(3)	0	1.92(6)
M3	Bi	.0191(5)	.1408(8)	0	1.56(7)
M4	Bi	.4891(5)	.3077(2)	1/2	4.00(9)
M5	Bi	.3430(5)	.4060(3)	0	5.90(9)
M6	Bi	.1582(4)	.2389(8)	1/2	1.50(7)
M7	Bi	.1535(4)	.9049(6)	1/2	.24(4)
M8	Bi	.0255(5)	.8082(2)	0	2.80(9)
M9	Bi	.4868(5)	.6411(8)	1/2	1.74(7)
M10	Bi	.1718(5)	.5717(9)	1/2	1.93(7)
M11	Bi	.0098(5)	.4748(8)	0	1.20(6)
M12	.7Pb+.3Bi	.3326(5)	.7521(2)	0	3.00(9)
Cu	.7Cu	.2455(20)	.6525(35)	0	5.00(85)
S1	.17Se+.83S	.2754(14)	.0179(20)	1/2	1.05(61)
S2	"	.1150(13)	.1018(21)	1/2	2.15(101)
S3	"	.0500(9)	.2958(19)	0	1.65(100)
S4	"	.0454(14)	.9600(17)	0	2.00(115)
S5	"	.4546(14)	.1291(20)	1/2	1.35(91)
S6	"	.3700(16)	.9370(21)	0	1.80(110)
S7	"	.2854(14)	.3515(25)	1/2	2.15(95)
S8	"	.3705(12)	.2684(21)	0	.95(92)
S9	"	.2200(11)	.1849(19)	0	1.06(85)
S10	"	.2056(14)	.5179(18)	0	1.85(101)
S11	"	.3795(15)	.6018(20)	0	2.14(102)
S12	"	.4549(9)	.7958(21)	1/2	1.44(95)
S13	"	.4546(14)	.4624(19)	1/2	1.85(95)
S14	"	.0550(13)	.6291(22)	0	1.65(87)
S15	"	.1205(10)	.4351(23)	1/2	.85(60)
S16	"	.2146(14)	.8520(23)	0	1.05(90)
S17	"	.1205(12)	.7684(24)	1/2	1.15(90)
S18	"	.1254(9)	.6849(21)	1/2	2.56(102)

TABLE 4. BOND LENGTHS IN PEKOITE

Cu	- S11	2.30 (10)		*M7* Bi7	- S5	2.55 (3)	
	- S18	2.33 (6)	X2		- S16	2.78 (5)	X2
	- S14	2.32 (5)			- S4	3.00 (4)	X2
M1 Bi1	- S6	2.64 (3)	X2		- S6	3.37 (3)	X2
	- S1	2.64 (4)		*M8* Bi8	- S16	2.63 (5)	
	- S4	3.10 (4)			- S17	2.65 (4)	X2
	- S2	3.09 (6)			- S5	3.03 (5)	
	- S1	3.53 (2)			- S8	3.14 (6)	
M2 Bi2	- S4	2.63(3)			- S9	3.51 (2)	
	- S1	2.78 (5)	X2	*M9* Bi9	- S11	2.70 (4)	X2
	- S5	3.12 (5)	X2		- S18	2.74 (4)	
	- S2	3.40 (3)	X2		- S15	2.99 (7)	
M3 Bi3	- S2	2.64(4)	X2		- S3	3.02 (5)	X2
	- S9	2.74 (4)			- S7	3.44 (2)	
	- S12	3.03 (5)	X2	*M10* Bi10	- S10	2.74(5)	X2
	- S6	3.13 (6)			- S13	2.74 (3)	
	- S16	3.50(2)			- S14	3.10 (5)	X2
M4 Bi4	- S8	2.76 (3)	X2		- S11	3.28 (3)	
	- S7	2.77 (5)		*M11* Bi11	- S10	2.68 (4)	
	- S17	2.98 (7)			- S15	2.73 (4)	X2
	- S14	3.03 (5)			- S13	2.99 (5)	X2
	- S18	3.41 (2)			- S11	2.99 (6)	
M5 Bi5	- S14	2.71(4)			- S10	3.50 (2)	
	- S7	2.80 (6)	X2	*M12* Pb1	- S12	2.86 (4)	X2
	- S13	3.05 (4)	X2		- S3	2.97 (4)	
	- S15	3.39 (2)			- S18	3.08 (5)	X2
M6 Bi6	- S12	2.61 (4)			- S17	3.20 (2)	X2
	- S9	2.80 (5)	X2				
	- S3	3.04 (4)	X2				
	- S8	3.31 (3)	X2				

As with gladite (Kohatsu & Wuensch 1973) and krupkaite (Synecek & Hybler 1975; Mumme 1975), pekoite demonstrates the tendency of Pb (and Cu) to order among as many distinct bismuthinite chains as possible.

The probe analyses given in Figure 1 (from Large & Mumme 1975, Table 8, Nos. 1,3,5,7 and 8) and the composition determined here for R27788 indicate that pekoite has a range of composition, and that the copper site in the structure may only be partially occupied with a necessary limited disordering of Pb and Bi atoms. On the other hand, analysis 6 (Table 8, Large & Mumme 1975) suggests a limited occupancy of copper atoms in excess of the ideal formula into other sites which are available to it in the structure — possibly those which are found to be fully occupied in gladite (Kohatsu & Wuensch 1973).

The disordering of the copper in the krupkaite ribbon has been discussed (Mumme 1975) and may also be a feature of all those derivative structures containing that ribbon — possibly it may even be direct evidence of transformation mechanisms which occur between members.

Similar solid-solution ranges to those of pekoite have now been reported in considerable detail by Harris & Chen (1976) for all members of the series except lindstromite ($Cu_3Pb_3Bi_7S_{15}$).

Crystal Structures of Synthetic Bismuthinite-Aikinite Members

Two previous studies of the members of the bismuthinite-aikinite series (Padera 1956; Springer 1971) were made using X-ray powder methods. Padera studied natural minerals whereas Springer studied synthetic members. Both described the system as a solid solution, an observation which in the case of Padera's work has not been supported by more recent studies. Although Springer's study was specifically directed towards the detection of superstructure formation in synthetic members, it was also carried out using powder X-ray methods. To obtain more direct information we attempted to prepare single crystals of various intermediate mem-

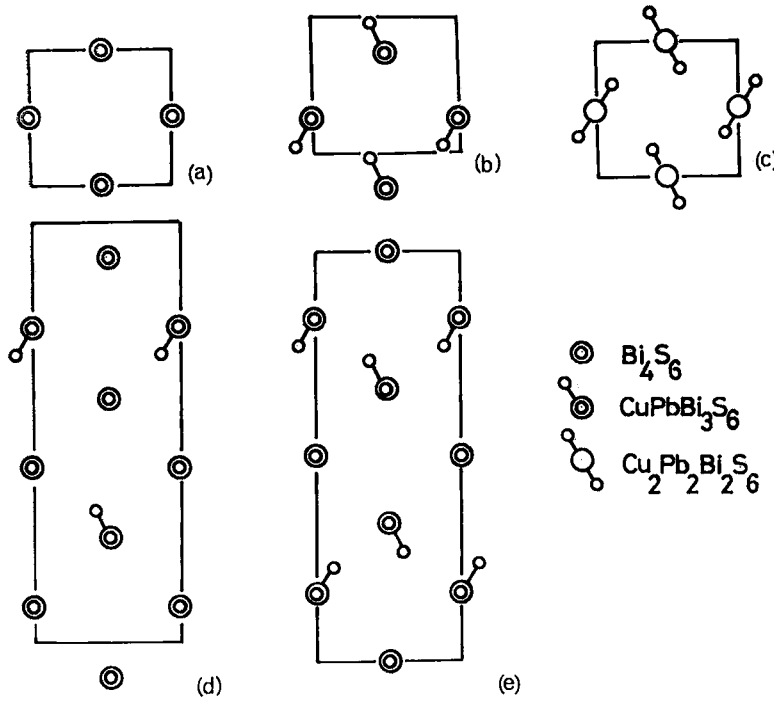

FIG. 5. Ribbon models for (a) bismuthinite, Bi_2S_3; (b) krupkaite, $CuPbBi_3S_6$; (c) aikinite, $CuPbBiS_3$; (d) pekoite, $CuPbBi_{11}S_{18}$; (e) gladite, $CuPbBi_5S_9$, in terms of the bismuthinite (Bi_4S_6), krupkaite ($CuPbBi_3S_6$) and aikinite ($Cu_2Pb_2Bi_2S_6$) ribbons.

bers of the series, and examined these by single-crystal methods.

Unfortunately, single crystals of a size necessary for manipulation were not obtained by our methods of preparation below 450°C, higher than Springer's lower limit of 300°C for compound formation. Nevertheless, the structures of the crystals prepared were studied, because it was considered possible that the limitations of the powder method to detect weak superlattice reflections may have influenced Springer's conclusions.

(1) *Experimental*

Synthetic members of the solid-solution series $CuPbBiS_3$–Bi_2S_3 were prepared using evacuated sealed silica tubes which were charged with the appropriate proportions of Bi_2S_3, Cu_2S and PbS previously prepared from pure elements. High-purity Koch-Light sulfur (99.9999%) was used together with A.R. lead and copper foils (metallic impurities <30 ppm) and high-purity Merck bismuth (<50 ppm total metallics). The tubes were placed into horizontal tube furnaces or muffles controlled within ±2°C of the set temperature with a proportional controller. They were left for periods of up to a week at temperature, after which they were rapidly quenched to the temperature of ice water. The products obtained from most of these reactions were polycrystalline, although in the synthesis of aikinite a macrocrystalline product was obtained from which single crystals were chosen for X-ray investigation. The preparation of the remaining phases were carried out by iodine-transport methods in sealed silica tubes containing 2-3 mg of I_2 per ml of tube volume, with temperature gradients of 500°-470°C. The bulk materials used for these experiments were prepared as outlined above, and after grinding were sealed under vacuum ($<10^{-4}$ atm), with the carefully weighed I_2, into the transport tubes.

Under the conditions of temperature gradient used for these experiments very little transport of the material took place, with the iodine acting as a vapor-phase medium for crystal growth of the bulk starting material which was set at 500°C and spread over 1-1½ cm from the end of the 12 cm-long tube. The reactions produced thin (<.02 mm) needle-like crystals approaching 0.3 mm in length and very suitable for single crystal X-ray diffraction analysis.

Quantitative chemical analyses of these vapor-

grown crystals showed that they contained less than 5 ppm iodine.

The products from the quenched reactions were examined by X-ray powder analysis using both a Philips diffractometer at a scanning rate of 1°/min., with Si powder as an internal standard, and a Guinier focusing camera with KCl as a standard. The unit cell at each composition was determined by a least-squares procedure. The lattice parameters of the single-crystal phases were determined from Guinier data using a small number of crushed crystals. These values were found to be in good agreement with parameters determined with the aid of a travelling microscope from unintegrated Weissenberg films for *a* and *c* and from rotation photographs for *b*.

Single-crystal X-ray analysis was undertaken at the following compositions (a) $Cu_{0.2}Pb_{0.2}Bi_{1.8}S_3$, (b) $Cu_{0.33}Pb_{0.33}Bi_{1.67}S_3$ (gladite), (c) $Cu_{0.5}Pb_{0.5}Bi_{1.5}S_3$ (krupkaite), (d) $Cu_{0.75}Pb_{0.75}Bi_{1.25}S_3$ and (e) $CuPbBiS_3$ (aikinite). Small needle-like crystals of the following dimensions were chosen for data collections: (a) $0.14\times0.03\times0.02$ mm; (b) $0.10\times0.05\times0.02$ mm; (c) $0.12\times0.04\times0.03$ mm; (d) $0.12\times0.04\times0.04$ mm and (e) $0.12\times0.03\times0.02$ mm for aikinite. Intensity data for the levels *h0l–h2l* were recorded on multiple films with Cu$K\alpha$ radiation using an integrating Weissenberg goniometer. The integrated intensities were corrected for Lorentz polarization and absorption using a linear absorption coefficient of 1380 cm^{-1} for Cu$K\alpha$ radiation. All calculations were made using an Elliott 803 computer with the aid of the programs of Daly *et al.* (1963). Scattering curves for neutral Pb, Bi, Cu and S were taken from the International Tables of Crystallography, Vol. III, with appropriate adjustment to the Cu scattering curve made at each composition. The initial atomic parameters for all atoms were taken from Kohatsu & Wuensch's (1971) data and the least squares refinement proceeded for all phases to give *R* factors of (a) 10.50% (b) 11.21%, (c) 9.57%, (d) 9.8%, and (e) 11.50% for aikinite. Isotropic temperature factors were used throughout the refinement.

(2) *Discussion of Results*

Powder data. As pointed out by Springer (1971) in his analysis of synthetic Bi_2S_3–$CuPbBiS_3$ members and also by Welin (1966) from his study of natural minerals which fell along this composition line, powder patterns taken across the series reveal a gradual but distinct change in line positions and intensity as the Pb content increases.

This is clearly demonstrated in a plot of Pb content versus the '*d*' value or $\sin^2\theta$ value of the 220 line for bulk preparations, as shown in

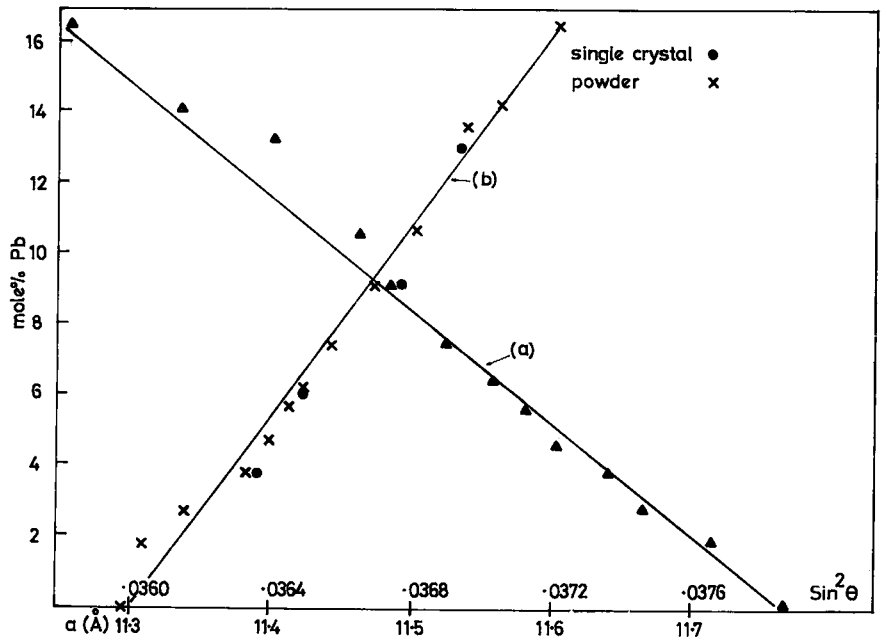

FIG. 6. (a) $\sin^2\theta$ values vs. Pb content for the 220 line of powder and ground single-crystal compositions Bi_2S_3-$CuPbBiS_3$; (b) lattice parameters *a* vs. Pb content for compositions Bi_2S_3-$CuPbBiS_3$.

Figure 6(a). Also included on this graph are the observed values for the 220 line obtained from Guinier data for powders ground from crystals grown by iodine transport. It clearly shows that the compositions of the crystals formed were consistent with those of the bulk starting materials, and this study of the powder data was primarily carried out to obtain this confirmation. The least-squares analysis of the powder data (Table 5) also confirms a gradual increase of all the lattice parameters with the replacement of Pb for Bi in Bi_2S_3 and the addition of Cu^{1+} to maintain the charge balance. The single-crystal data (Table 6) also show this trend which gives an overall increase in cell volume of 30.1Å^3 from Bi_2S_3 to $CuPbBiS_3$. Figure 6(b) indicates the linear relationship between the *a* lattice parameter and the lead content. Careful examination of the Guinier data for all compositions showed no indication of superlattice reflections, in agreement with Springer's (1971) observations.

Single crystal analysis. None of the Weissenberg films revealed superlattice formation at any of the intermediate compositions examined. All of the crystals had lattice parameters intermediate between bismuthinite and aikinite, and all had space group *Pnma*.

A complete description and comparison of the structures of aikinite and bismuthinite has been given by Kohatsu & Wuensch (1971) and a comparison of their lattice parameters, bond lengths, and atomic coordinates with our synthetic aikinite is given in Tables 6-8. These clearly indicate that aikinite prepared from pure Cu,Bi, and Pb sulfides at 500°C is in all respects identical with the natural mineral. Aikinite is an expanded version of bismuthinite; lead substitutes in an ordered manner for bismuth in the *M*(2) site of bismuthinite and copper atoms occupy the tetrahedral sites.

A comparison of bond distances for the synthetic intermediates is shown in Table 7, which refers to the drawing of the unit cell in Figure 7. There is a small change in bond lengths for Cu-S(1), even when the large *e.s.d.*'s of the $Cu_{0.2}$ phase are considered. The variation in the Cu-S(3) and Cu-S(2) distance is very small, but for Cu-S(2) there is an apparent sharp increase of 0.13Å from the $Cu_{0.2}$ composition to the $Cu_{0.33}$ phase.

The *M*(2) site has seven nearest neighbor sulfur atoms and their bond distances are shown in Table 7(b). The change in lengths for *M*(2)–S(1) bonds of 2.58Å to 2.85Å from Bi_2S_3 to $CuPbBiS_3$ confirms that lead progressively replaces bismuth in the *M*(2) sites, not in the *M*(1) sites. The *M*(2)–S(3)^1 distances show a corresponding increase as lead replaces bismuth.

TABLE 5. LATTICE PARAMETERS OF INTERMEDIATE MEMBERS FROM POWDER DATA*

Composition	*a*(Å)	*b*(Å)	*c*(Å)
Bi_2S_3	11.294(7)	3.979(6)	11.143(7)
$Cu_{0.1}Pb_{0.1}Bi_{1.9}S_3$	11.309(8)	3.987(7)	11.149(8)
$Cu_{0.14}Pb_{0.14}Bi_{1.86}S_3$	11.341(10)	3.988(8)	11.164(9)
$Cu_{0.2}Pb_{0.2}Bi_{1.8}S_3$	11.385(8)	4.018(8)	11.195(7)
$Cu_{0.25}Pb_{0.25}Bi_{1.75}S_3$	11.401(7)	4.021(6)	11.217(6)
$Cu_{0.30}Pb_{0.30}Bi_{1.70}S_3$	11.412(8)	4.019(5)	11.220(7)
$Cu_{0.33}Pb_{0.33}Bi_{1.67}S_3$	11.425(9)	4.021(7)	11.238(8)
$Cu_{0.4}Pb_{0.4}Bi_{1.6}S_3$	11.445(8)	4.022(6)	11.258(10)
$Cu_{0.5}Pb_{0.5}Bi_{1.5}S_3$	11.482(8)	4.024(5)	11.268(8)
$Cu_{0.6}Pb_{0.6}Bi_{1.4}S_3$	11.506(10)	4.026(7)	11.276(7)
$Cu_{0.75}Pb_{0.75}Bi_{1.25}S_3$	11.535(10)	4.026(7)	11.276(4)
$Cu_{0.8}Pb_{0.8}Bi_{1.2}S_3$	11.537(11)	4.027(8)	11.287(6)
$Cu_{0.86}Pb_{0.86}Bi_{1.14}S_3$	11.565(10)	4.029(6)	11.293(9)
$Cu_{1.0}Pb_{1.0}Bi_{1.0}S_3$	11.602(9)	4.034(7)	11.305(5)

*esd in parentheses

TABLE 6. LATTICE PARAMETERS OF SINGLE CRYSTALS OF INTERMEDIATE MEMBERS*

Composition	*a*(Å)	*b*(Å)	*c*(Å)	Vol. (Å)^3
$Cu_{0.0}Pb_{0.0}Bi_2S_3$†	11.282	3.971	11.112	497.826
$Cu_{0.2}Pb_{0.2}Bi_{1.8}S_3$	11.392(6)	4.014	11.222(5)	513.17
$Cu_{0.33}Pb_{0.33}Bi_{1.67}S_3$	11.422(3)	4.018(5)	11.224(6)	515.10
$Cu_{0.5}Pb_{0.5}Bi_{1.5}S_3$	11.495(6)	4.022(4)	11.264(5)	520.81
$Cu_{0.75}Pb_{0.75}Bi_{1.25}S_3$	11.535(10)	4.026(7)	11.276(4)	523.65
$Cu_{1.0}Pb_{1.0}Bi_{1.0}S_3$	11.603(7)	4.031(6)	11.301(5)	528.52
$CuPbBiS_3$††	11.6083(10)	4.0279(3)	11.2754(17)	527.20

*esd in parentheses.
†Kupcik & Vesela-Novakova (1970).
††Naturally occurring aikinite (Kohatsu & Wuensch 1971).

TABLE 7. INTERATOMIC DISTANCES

(a) Cu

Composition	S1	S3^{1}x2	S2
$Cu_{0.2}Pb_{0.2}Bi_{1.8}S_3$	2.22(8)	2.38(4)	2.29(2)
$Cu_{0.33}Pb_{0.33}Bi_{1.67}S_3$	2.23(6)	2.38(3)	2.42(1)
$Cu_{0.5}Pb_{0.5}Bi_{1.5}S_3$	2.25(6)	2.36(3)	2.38(2)
$Cu_{0.75}Pb_{0.75}Bi_{1.25}S_3$	2.31(3)	2.37(1)	2.43(1)
$Cu_{1.0}Pb_{1.0}Bi_{1.0}S_3$	2.31(3)	2.38(1)	2.43(2)
$Cu_{1.0}Pb_{1.0}Bi_{1.0}S_3$††	2.31(1)	2.37(1)	2.43(1)

(b) *M*(2)=[Pb,Bi]

Composition	S1	S3^{1}x2	S1^{1}x2	S2^{1}x2
Bi_2S_3†	2.58	2.74	2.97	3.33
$Cu_{0.2}Pb_{0.2}Bi_{1.80}S_3$	2.64(3)	2.82(2)	3.01(1)	3.34(2)
$Cu_{0.33}Pb_{0.33}Pb_{1.67}S_3$	2.69(3)	2.81(1)	2.95(1)	3.35(2)
$Cu_{0.5}Pb_{0.5}Bi_{1.5}S_3$	2.67(2)	2.85(1)	3.00(1)	3.35(1)
$Cu_{0.75}Pb_{0.75}Bi_{1.25}S_3$	2.83(1)	2.89(1)	2.98(1)	3.28(1)
$Cu_{1.0}Pb_{1.0}Bi_{1.0}S_3$	2.85(1)	2.92(1)	2.99(1)	3.27(1)
$Cu_{1.0}Pb_{1.0}Bi_{1.0}S_3$	2.84(1)	2.95(1)	2.98(1)	3.28(1)

(c) *M*(1)=[Bi]

Composition	S3	S2^{1}x2	S1^{111}x2	S2^{11}	S3^{11}
Bi_2S_3†	2.63	2.62	3.06	3.05	3.47
$Cu_{0.2}Pb_{0.2}Bi_{1.8}S_3$	2.69(3)	2.70(2)	3.00(2)	3.09(1)	3.41(2)
$Cu_{0.33}Pb_{0.33}Bi_{1.67}S_3$	2.68(2)	2.70(2)	3.06(1)	3.02(1)	3.47(2)
$Cu_{0.5}Pb_{0.5}Bi_{1.5}S_3$	2.72(1)	2.70(2)	3.05(1)	3.10(1)	3.44(2)
$Cu_{0.75}Pb_{0.75}Bi_{1.25}S_3$	2.67(1)	2.74(1)	2.99(1)	3.05(1)	3.52(1)
$Cu_{1.0}Pb_{1.0}Bi_{1.0}S_3$	2.68(1)	2.76(1)	2.97(1)	3.07(2)	3.53(1)
$Cu_{1.0}Pb_{1.0}Bi_{1.0}S_3$††	2.66(1)	2.73(1)	2.97(1)	3.12(1)	3.53(1)

†Kupcik & Vesela-Novakova (1970) ††Kohatsu & Wuensch (1973)

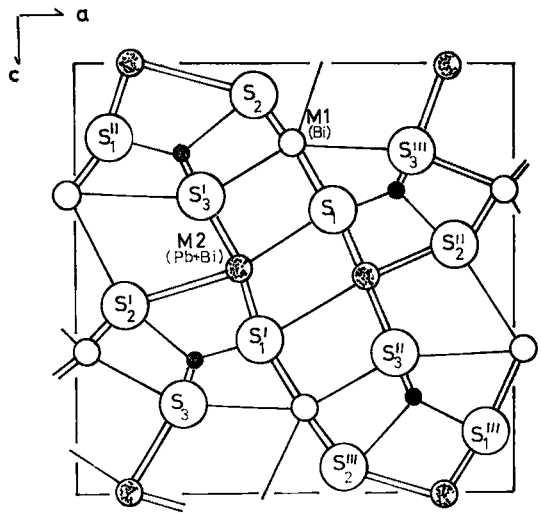

FIG. 7. The crystal structure of aikinite projected onto (010). Labelling of atoms is that referred to in the text.

Figure 8 shows a plot of these two distances versus composition. There appears to be a linear relationship for the $M(2)$–S(3) distance, with a maximum value of 2.92Å at the limiting composition. The $M(2)$–S(1) distances exhibit a similar relationship. The $M(2)$–S(1)[1] and $M(2)$–S(2)[1] distances vary only slightly, by 0.07Å, over the whole composition range.

The $M(1)$–S coordination polyhedron (Table 7, Fig. 7) forms a severely distorted octahedron with a seventh sulfur 0.5Å distant from the next-nearest neighbor. These bond distances show relatively small changes from Bi_2S_3 through to $CuPbBiS_3$, the only significant change being for the $M(1)$–S(2)[1] distance which increases from 2.62Å in Bi_2S_3 to 2.76Å in aikinite, but more than half this increase takes place between Bi_2S_3 and $Cu_{0.2}Pb_{0.2}Bi_{1.80}S_3$.

There is a small non-linear increase at $Cu_{0.5}$ for the $M(1)$–S_3 distance. The increase from 2.68Å at the $Cu_{0.33}$ composition to a maximum of 2.72Å at the $Cu_{0.5}$ phase and back to 2.66Å at pure aikinite may be related to the decrease of 0.02Å in the $M(2)$–S(1) distance at the same composition, suggesting some slight disorder of the Pb and Bi in the $M(1)$ sites. As no evidence of superstructure formation was observed, the results of this investigation indicate that, under the conditions that the phases were formed, the copper atoms tend to fill the tetrahedral holes progressively, and at the same time there is an ordered replacement of bismuth by lead in the $M(2)$ sites of the structure.

FORMATION OF BISMUTHINITE DERIVATIVES

This study of the synthetic bismuthinite-aikinite system has confirmed Springer's (1971) claim that, at least at 450-500°C, complete solid solution exists between the end members. It should be noted that Springer's results could be interpreted to indicate the formation either

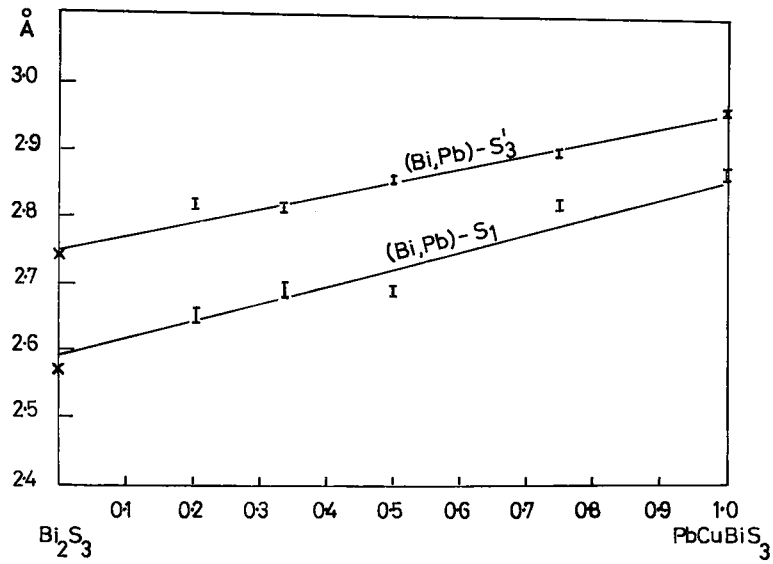

FIG. 8. Graphs showing the variation of $M(2)$-S(3)[1] and $M(2)$-S(1) bond distances in composition Bi_2S_3-$CuPbBiS_3$. Estimated standard deviations are indicated by line bars.

of a complete solid-solution series, or of a series of compositions based on a *disordered structure type* in which lead and bismuth atoms statistically occupy the atomic positions available to them in the bismuthinite structure. As less disordering would be expected at lower temperatures, the partial ordering behavior observed in this study must be considered to continue to lower temperatures where it is known that the fully ordered phases are stable.

Exsolution textures have been reported in the minerals of this series by Ramdohr (1969), but Welin (1966) was the first to support his observations of these phenomena with quantitative results. In RM24099 he reported a member with 5% Cu, 20% Pb, 56% Bi and 19% S (probably krupkaite) containing exsolved bismuthinite. In another two crystals of RM24100, he observed similar exsolution textures; probe analysis made on the host mineral in one gave results close to the composition of gladite. Correia Neves *et al.*, (1974) and Harris & Chen (1976) have also reported quantitative exsolution studies which, together with the results of the present work, firmly establish an immiscibility between pekoite and gladite.

Intergrowths among the minerals of the series have also been examined and described in some detail. These are intergrowths of bismuthinite/krupkaite; bismuthinite/gladite; and less frequently, bismuthinite/gladite/krupkaite — all reported by Zak *et al.* (1975) — and Karup-Møller (1972) has described a bismuthinite/"lindstromite" (probably krupkaite)/pavonite intergrowth.

Attempts to prepare single crystals of gladite, pekoite or krupkaite below 400°C were not successful. Very limited crystal growth was obtained and the powder patterns corresponded to the solid-solution members. No superlattice reflections were observed on any of the Guinier photographs. Attempts to anneal at 300-350°C crystals that have been prepared at temperatures greater than 450°C are currently being undertaken.

Unless examination of single crystals prepared at various temperatures below 450° shows otherwise, Springer's limit of 300°C must be accepted as approximately representing the maximum temperature at which natural pekoite *etc.* have been formed. Either there has occurred a slow cooling process with unmixing and segregation from an original solid solution at or below 300°C, or there has been direct formation by some other ore-forming process.

Supported by the now well-established evidence of the pekoite/gladite exsolutions, one might expect that all individual solvi in the system would be as is represented diagrammatically in Figure 9, which is drawn in the style of Harris & Chen (1976). The pekoite/gladite exsolution proves that these two minerals have been deposited (or at least existed) as a solid solution, and Harris & Chen (1976) give good evidence that the final quenching of these may have taken place at different temperatures in different cases.

However, the coexistence of krupkaite and bismuthinite (Welin 1966) as exsolutions and the intergrowths reported by Zak *et al.* (1975) and Karup-Møller (1972), are difficult to explain on the basis of simple immiscibility gaps, and could suggest much more complicated phase relationships. On the other hand, the coexistence of these minerals may be good evidence that all were formed *directly* at low temperatures, perhaps at different stages in the mineralization process.

Classification of Superstructures

Previous attempts to classify the ordered mineral phases in terms of a general formula have proved unsuccessful in terms of predicting the structures of all the known members. However, based on present knowledge of the series,

TABLE 8. ATOMIC COORDINATES*

Atom		Bi_2S_3 †	$Cu_{.2}Pb_{.2}Bi_{1.8}S_3$	$Cu_{.33}Pb_{.33}Bi_{1.667}S_3$	$Cu_{.5}Pb_{.5}Bi_{1.5}S_3$	$Cu_{.75}Pb_{.75}Bi_{1.25}S_3$	$CuPbBiS_3$	$CuPbBiS_3$ ††
$Bi_{(1)}$	x	0.0168	0.0165(3)	0.0157(3)	0.0167(4)	0.0169(3)	0.0175(3)	0.0185(2)
	z	0.6741	0.6762(4)	0.6771(4)	0.6767(3)	0.6780(3)	0.6802(4)	0.6812(2)
$Pb_{(Bi)}$	x	0.3407	0.3398(4)	0.3386(4)	0.3398(4)	0.3335(4)	0.3342(4)	0.3332(2)
	z	0.4660	0.4701(5)	0.4726(4)	0.4720(4)	0.4839(4)	0.4864(3)	0.4880(3)
Cu	x	-	0.2324(41)	0.2308(39)	0.2297(15)	0.2355(10)	0.2347(22)	0.2320(8)
	z	-	0.2011(40)	0.2075(38)	0.2062(20)	0.2089(11)	0.2076(24)	0.2081(9)
S_1	x	0.0486	0.0488(21)	0.0516(20)	0.0481(11)	0.0487(10)	0.0471(12)	0.0454(9)
	z	0.1300	0.1345(22)	0.1291(19)	0.1313(10)	0.1363(20)	0.1389(11)	0.1373(11)
S_2	x	0.3785	0.3770(24)	0.3813(20)	0.3772(12)	0.3807(10)	0.3784(12)	0.3795(9)
	z	0.0576	0.0615(24)	0.0548(17)	0.0585(17)	0.0522(7)	0.0514(13)	0.0553(10)
S_3	x	0.2169	0.2164(20)	0.2136(21)	0.2185(15)	0.2123(8)	0.2128(14)	0.2146(9)
	z	0.8062	0.8027(19)	0.8056(19)	0.8032(17)	0.8055(19)	0.8054(12)	0.8036(9)

*esd in parenthesis †Kupcik & Vesela-Novakova (1970) ††Kohatsu & Wuensch (1973).

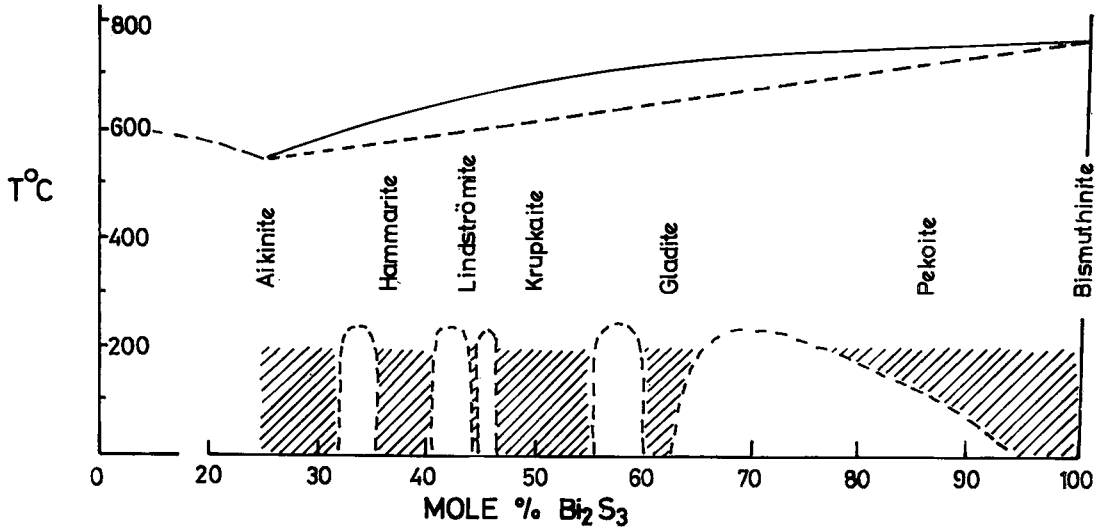

FIG. 9. Compositional ranges (see Harris & Chen 1976) in terms of mole % Bi_2S_3 and suggested subsolidus phase relationships in the system Bi_2S_3-$CuPbBiS_3$. The liquidus and solidus are from Springer (1971).

it is possible to represent the ideal composition of all of the ordered members between bismuthinite and krupkaite by the formula $Cu_xPb_xBi_{12-x}S_{18}$, where $x = 0$ for bismuthinite, $x = 1$ for pekoite, $x = 2$ for gladite, and $x = 3$ for krupkaite. Two of the other known members between krupkaite and aikinite may also be represented by this formula. These are hammarite, for which $x = 4$, and aikinite, for which $x = 6$. Welin's lindstromite, $Cu_3Pb_3Bi_7S_{15}$, with a subcell 5 times that of bismuthinite, is the only member of the series which does not satisfy this simple classification and apparently does not have an extensive solid-solution range (Harris & Chen 1976).

The reason for this apparent exception must be sought in the crystal structure of lindstromite, and classification of the system can be further clarified only as the structure of it and any additional members are determined — though judging by the solid-solution ranges presented by Harris & Chen (1976) there is little scope for this. The use of distinct names for the ordered members of the sequence is to be encouraged, as it emphasizes the real nature of the composition series.

REFERENCES

BUSING, W. R., MARTIN, K. O. & LEVY, H. A. (1962): ORFLS, a Fortran crystallographic least-squares program. *U.S. Nat. Tech. Inf. Serv. ORNL-TM-305.*

CORREIA NEVES, J. M., LOPES NUNES, J. E., SAHAMA, TH. G., LEHTINEN, M. & KNORRING, O. V. (1974): Bismuth and antimony minerals in the granite pegmatites of Northern Mosambique. *Rev. Cienc. Geol., Lourenco Marques* 7, Ser. A, 1-37.

CRUICKSHANK, D. W. J., PILLING, P. E., BUJOSA, A., LOVELL, F. M. & TRUTER, M. R. (1961): Computing methods and the phase problem. In *X-roy Crystal Analysis.* Pergamon Press, Oxford.

DALY, J. J., STEPHENS, F. S. & WHEATLEY, P. J. (1963): Monsanto Research, S.A., Final Report No. 52.

HARRIS, D. C. & CHEN, T. T. (1976): Crystal chemistry and re-examination of nomenclature of sulfosalts in the aikinite-bismuthinite series. *Can. Mineral.* 14, 194-205.

ITO, T. (1973): On the application of a minimum residual method to the structure determination of super structures. *Z. Krist.* 137, 399-411.

KARUP-MØLLER, S. (1972): New data on pavonite, gustavite and some related sulphosalt minerals. *Neues Jahrb. Mineral. Abh.* 117, 19-37.

KUPCIK, V. & VESELA-NOVAKOLA, L. (1970): The crystal structure of bismuthinite redetermined. *Tschermaks Mineral. Petrog. Mitt.* 14, 55-58.

KOHATSU, I. & WUENSCH, B. J. (1971): The crystal structure of aikinite $PbCuBiS_3$. *Acta Cryst.* B27, 1245-1252.

——— & ——— (1973): The crystal structure of gladite, $PbCuBi_5S_9$. *Amer. Mineral.* 58, 1098 (Abstr.).

LARGE, R. R. (1974): *Gold, Bismuth, Copper, Selenium Mineralization in the Tennant Creek*

District, Central Australia. Ph.D. thesis, Univ. New England, New South Wales.

——— & MUMME, W. G. (1975): Junoite, "wittite" and related seleniferous bismuth sulfosalts from Juno Mine, Northern Territory, Australia. *Econ. Geol.* **70**, 369-383.

MOORE, P. B. (1967): A classification of sulfosalt structures derived from the structure of aikinite. *Amer. Mineral.* **52**, 1874-1876.

MUMME, W. G. (1975): The crystal structure of krupkaite, $CuPbBi_3S_6$, from the Juno mine at Tennant Creek, Northern Territory, Australia. *Amer. Mineral.* **60**, 300-308.

———, WELIN, E. & WUENSCH, B. J. (1976): Crystal chemistry and proposed nomenclature for sulfosalts intermediate in the system bismuthinite-aikinite (Bi_2S_3-$CuPbBiS_2$) *Amer. Mineral.* **61**, 15-20.

OHMASA, M. & NOWACKI, W. (1970): Note on the space group and on the structure of aikinite derivatives. *Neues Jahrb. Mineral. Monatsh.* 158-162.

PADERA, K. (1956): Beitrag Zur Revision der Mineralien aus der Gruppe von Wismutglanz und Aikinit. *Chem. Erde* **18**, 14-18.

RAMDOHR, P. (1969): *The Ore Minerals and Their Intergrowths,* 3rd ed., Pergamon, Oxford.

SYNECEK, V. & HYBLER, J. (1975): The crystal structures of krupkaite, $CuPbBi_3S_6$, and of gladite, $CuPbBi_5S_9$, and the classification of superstructures in the bismuthinite-aikinite group. *Neues Jahrb. Mineral. Monatsh.*, 541-560.

SPRINGER, G. (1971): The synthetic solid-solution series Bi_2S_3-$BiCuPbS_3$ (bismuthinite-aikinite). *Neues Jahrb. Mineral. Monatsh.*, 19-24.

WELIN, ERIC (1966): Notes on the mineralogy of Sweden. 5. Bismuth-bearing sulphosalts from Gladhammer, a revision. *Ark. Mineral. Geol.* **4**, 377-386.

ZAK, L., SYNECEK, V. & HYBLER, J. (1975): Krupkaite, $CuPbBi_3S_6$, a new mineral of the bismuthinite-aikinite group. *Neues Jahrb. Mineral Monatsh.*, 533-541.

Manuscript received January 1976, emended March 1976.